Published in final edited form as:
Eur J Pharmacol. 2011 April 25; 657(1-3): 159–166. doi:10.1016/j.ejphar.2011.01.060.

Tumor Necrosis Factor-α induces increased lung vascular permeability: a role for GSK3α/β

Amy Barton-Pai[*], **Carlos Feleder**[#], and **Arnold Johnson**[#]

[#] Department of Pharmaceutical Science, Albany College of Pharmacy and Health Sciences, Albany, N.Y. 12208

[*] Department of Pharmacy Practice, Albany College of Pharmacy and Health Sciences, Albany, N.Y. 12208

Abstract

We tested the hypothesis that glycogen synthase kinase 3α/β (GSK3α/β) modulates tumor necrosis factor-a (TNF) induced increased lung vascular permeability. Rats were treated with TNF (i.v., ~100 ng/ml) or vehicle 0.5 h, 4.0 h and 24.0 h prior to lung isolation. Rats were co-treated with the GSK3α/β inhibitors SB216763 (0.6 mg/kg) or TDZD-8 (1.0 mg/kg). After TNF, the isolated lung was assessed for hemodynamics, wet-dry/dry weight (W-D/D) and extravascular albumin. Extravascular albumin significantly increased at TNF-24 h compared to Control. In the GSK3α/β-inhibited +TNF groups, extravascular albumin was similar to the Control and respective SB216763 and TDZD-8 groups. In separate studies, to assess GSK3α/β-activity, lung lysate was assessed for phospho-GSK3α/β-Ser$^{21/9}$, total GSK3α/β, un-phospho-β-catenin-Ser$^{33/37}$and total β-catenin. In the TNF-4.0 h group, there was no change in GSK3α/phospho-GSK3α-Ser^{21} but there was an increase in GSK3β/GSK3β-Ser^{9} compared to Control, indicating GSK3β activation at TNF-4.0 h. GSK3β activation was verified because there was a decrease in un-phospho-β-catenin-Ser$^{33/37}$/β-catenin in the TNF- 4.0 group, a specific outcome for GSK3β activation. In the SB216763+TNF group, un-phospho-β-catenin-Ser$^{33/37}$ was similar to Control, indicating prevention of TNF-induced GSK3β activation. In the TNF-24 h group, there were increases in the biomarkers of inflammation phospho-eNOS-Ser ^{1117} and oxidized protein, which did not occur in the SB216763+TNF-24 h and TDZD-8+TNF-24 h groups. In the SB216763+TNF-24 h and TDZD-8+TNF-24 h groups, un-phospho-β-catenin-Ser$^{33/37}$ was greater than in the Control, indicating continued inhibition of GSK3β. The data indicates that pharmacologic inhibition of GSK3β inhibits TNF induced increased endothelial permeability associated with lung inflammation.

Index words

edema; inflammation; lung injury; β-catenin; glycogen synthase kinase; permeability

Corresponding Address: Arnold Johnson, Ph.D., Professor, Department of Pharmaceutical Science, Albany College of Pharmacy and Health Science, Room 104D BRB, Albany NY 12208, arnie.johnson@acphs.edu.

1. INTRODUCTION

Glycogen synthase 3 (GSK3) is a serine/threonine kinase with two isoforms α and β (Bhat et al., 2004; Dugo et al., 2007b; Miura and Miki, 2009). The Akt-mediated phosphorylation of GSK3α/β-$Ser^{21/9}$ *in vitro* suppresses the activity of GSK3α/β (Aberle et al., 1997; Daugherty and Gottardi, 2007). GSK3α/β targets a variety of proteins for serine phosphorylation (Bhat et al., 2004; Dugo et al., 2007b; Miura and Miki, 2009). β-catenin (Aberle et al., 1997) is a cytoskeletal protein affecting lung permeability that is significantly targeted by GSK3α/β. GSK3α/β mediated phosphorylation of β-catenin-$Ser^{33/37}$ targets β-catenin for ubiquination and degradation by the proteosome (Aberle et al., 1997). Conversely, the inhibition of GSK3α/β decreases phosphorylation of β-catenin-$Ser^{33/37}$ which promotes β-catenin translocation to the peripheral membrane and nucleus associated with β-catenin mediated transcription of genes (Hagen et al., 2002; Laux et al., 2004; Lee et al., 2008; Masckauchan et al., 2006; Schafer et al., 2003).

TNF is a mediator of Acute Respiratory Distress Syndrome and sepsis syndrome (Eichacker et al., 1991; Fujisawa et al., 1998). The GSK3α/β affected pathways, β-catenin and reactive oxygen/nitrogen species, are within the paradigm of TNF-induced alterations in lung permeability and the associated inflammatory response (Cuzzocrea et al., 2006; Dugo et al., 2007a; Dugo et al., 2007b; Huang et al., 2009). We demonstrated both *in vitro* and *in vivo* that reactive nitrogen species mediates the TNF induced endothelial barrier dysfunction, and *in vitro* both the associated increased nitrotyrosine (i.e., protein nitration) and protein-carbonyls (i.e., protein oxidation) (Ferro et al., 1997; Neumann et al., 2006).

TNF *in vivo* causes increased vascular permeability of the isolated lung (Hocking et al., 1990; Johnson and Ferro, 1996); however, the role of GSK3α/β in the pulmonary response to TNF is not known. Thus, we tested the hypothesis that there is increased activation of GSK3α/β in isolated lungs of rats treated with TNF. In addition, we tested the idea that the GSK3α/β inhibitors SB216763 and TDZD-8 prevent TNF-induced increases in: (1) phosphorylation of β-catenin-$Ser^{33/37}$ (i.e., a biomarker for GSK3α/β activity, (2) endothelial barrier dysfunction (i.e., a marker of lung injury), and (3) oxidized protein (i.e., a marker of lung inflammation).

2. MATERIALS and METHODS

2.1. Reagents

All reagents are obtained from Sigma Chemical Company (St. Louis, MO) unless otherwise noted. Highly purified recombinant human TNF from *E. coli* (American Research Products, Belmont, MA) was used as previously indicated (Gertzberg et al., 2004; Neumann et al., 2006). The endotoxin level was less than 0.1 ng/μg of TNF. We previously showed that boiling TNF for 0.75 h blocks the effect of TNF in our system (Ferro et al., 1993) which indicates no endotoxin contamination.

2.2. *In vivo* treatments

Rats (Male Spraque-Dawley, 225–300 g; Charles River Laboratories, Wilmington, Mass) were anesthetized with isoflurane (4 % for induction and 1.5 % for maintenance) in 100% O_2. The rats were treated with TNF (600 ng/100 gm) via intravenous tail vein injection 0.5 h, 4.0 h and 24.0 h prior to lung isolation. The initial blood [TNF] is assumed to be ~ 100 ηg/ml by using a blood volume = Body Weight × 0.06 (Lee and Blaufox, 1985). Rats were treated with this dose of TNF because our previous work shows this dose induces a consistent increase in lung microvessel endothelial cell monolayer albumin permeability (Bove et al., 2001; Gertzberg et al., 2004; Neumann et al., 2006). In separate studies, the ATP competitive GSK-3α/β antagonist SB216763 [0.6 mg/kg; 3-(2,4-Dichlorophenyl)-4-(1-

methyl-1H-indol-3-yl)-1H-pyrrole-2,5-dione] (Biomol, Plymouth Meeting, PA) was used (Dugo et al., 2007b; Meijer et al., 2004). In addition, the GSK-3β specific non-ATP competitive antagonist TDZD-8 (1 mg/kg; 4-Benzyl-2-methyl-1,2,4-thiadiazolidine-3,5-dione) was used (Cuzzocrea et al., 2006; Meijer et al., 2004). The SB216763 and TDZD-8 was injected with the TNF. All studies were approved by the IACUC of the Albany VA Medical Center.

2.3. Isolated Perfused Lung

The isolated perfused rat lung studies were performed using a modification of our technique (Ferro et al., 1993; Johnson and Ferro, 1992; 1996). Rats were anesthetized with a cocktail of ketamine (0.5 mg/kg), xylazine (5 mg/kg) and acepromazine (1 mg/kg). The trachea was cannulated and the chest was opened by median sternotomy. Heparin (7 U/10 g body weight, Abraxis Pharmaceutical, Schaumberg, IL) was administered by intracardiac puncture injection. The lungs and heart were excised and suspended from a force displacement transducer (model TSD105A, Harvard Apparatus, Holliston, MA). The airway pressure was maintained at 1 cm H_20 with room air throughout the experiment. The pulmonary artery and left atrium were cannulated, and the left atrial pressure was set at 4 cmH_20. Lung perfusion (0.04 ml/min/g body weight) [Q]) was maintained by a peristaltic roller perfusion pump (model 7523-60 & 7518, Cole-Palmer, Vernon Hills, IL). The recirculation of perfusate (150 ml) was begun after the venous effluent was clear of cellular elements. The perfusate is phosphate buffered Ringer's solution with 5.55 mM dextrose and 3.0 g/100 ml bovine serum albumin (fraction V). The system was maintained at a constant temperature of 36°C–37°C, and the pH was maintained between 7.35 and 7.45. The pulmonary artery pressure (Ppa) was monitored using a pressure catheter (PE-50) inserted into the pulmonary artery cannula and connected to a pressure transducer (model TSD104A, Harvard Apparatus). The pulmonary venous pressure (Ppv) was monitored similarly except that the pressure catheter was inserted into the left atrial catheter. The Ppa, Ppv, and change in weight were recorded continuously (model MP100 w/Acknowledge Software, BioPac Systems, Inc., Goleta, CA). Lungs were excluded from study if there was a spontaneous increase in Ppa, Ppv or weight occurred during the 15 min baseline perfusion period following lung isolation.

2.4. Pulmonary Capillary Pressure, Pulmonary Arterial Resistance and Pulmonary Venous Resistance

Pulmonary capillary pressure (Ppc) was estimated using the double occlusion method as previously described (Ferro et al., 1993; Johnson and Ferro, 1992; 1996). The arterial inflow and venous outflow lines were simultaneously occluded using in-line solenoid valves, and the Ppc was estimated by measuring the subsequent equilibrium pressure. The Ppc estimate was used to determine both the pulmonary arterial resistance (Ra) and pulmonary venous resistance (Rv) from the equations $Ra=(Ppa-Ppc)/Q$ and $Rv=(Ppc-Ppv)/Q$.

2.5. Lung (Wet-Dry)-to-Dry Weight Ratio

At the end of the experiment, the lungs were removed, cleared of all extra pulmonary tissue and weighed as previously done by us (Johnson and Ferro, 1992; 1996). After the lungs were dried at 110°C overnight, they were weighed and the wet-dry/dry weight ratio (W-D/D) was calculated.

2.6. Lung extravascular protein flux

Protein flux was assessed using the extra vascular accumulation of albumin-FITC (Cuzzocrea et al., 2006). In separate studies, the lung was perfused with the phosphate buffered Ringer's (200 ml) as described above. The baseline Ppc was determined following

the stable perfusion period. The lung was then perfused (~ 5 min) with a phosphate buffered Ringer's (100 ml)-FITC-BSA solution (800 μl of 20 mg/ml) after the measurement of the baseline Ppc. Then a "washout" of intravascular FITC-BSA was done with the phosphate buffered Ringer's (200 ml) achieving a perfusate with no detectable FITC-BSA. The lungs were then dried and homogenized in sterile water. The homogenate was centrifuged at 18,000 g for 30 min at 4°C. The supernatant was retrieved and stored at 4°C. We are confident that the extravascular albumin represents tissue protein because: (1) the lung lysate is prepared following washout of the FITC-albumin, (2) the TCA-precipitated perfusate and lysate free/bound ratio of FITC-albumin is 0 %, (3) tissue autofluorescence is corrected by subtracting fluorescence values using a non-albumin-FITC treated lung, (4) fluorescence values are verified with immuno-detection of intact FITC-albumin only at the correct MW of 66.4 kD as shown below, and (5) vascular binding of FITC-albumin should be minimal because the unlabeled albumin is 187 times the concentration of the FITC-albumin

A FITC-BSA standard curve (0–100 ηM) and samples were prepared in 10 mM Tris buffer (pH 8.0). The samples were placed in a 96 well black plate (Corning Costar, Corning, NY) and fluorescence determined (Wallac 1420 Victor 2, Perkin-Elmer, Waltham, MA). The samples were corrected for autofluorescence (i.e., the negative control) using a non-FITC mediated signal from a lung that was only perfused with the phosphate buffered Ringers. The FITC signal was corrected for the mass of the samples by a lung protein determination with BCA (Thermo Scientific, Pierce, Rockford, Il) using a spectrophotometer (Spectra Max Plus, Micro plate Molecular Devices, Sunnyvale, CA). The intact FITC-albumin fluorescence was verified with immuno-detection of the 66.7 kDa FITC-albumin using anti-FITC

2.7. Lung Tissue Collection and Homogenization

Lungs were isolated as described above, and perfused with buffered Ringer's solution and albumin (~100 ml) to clear the vascular bed of blood components. Lungs were then immediately diced into ~3 mm pieces, frozen in liquid nitrogen, and stored at −80°C for later homogenization. Frozen lung tissue was homogenized on ice with a Bio Homogenizer M 133/1281-0 (Biospec Products, Inc., Bartlesville, OK) in 15 ml glass centrifuge tubes (Corex No.8441, Corning Costar, Corning, NY). Between 150–200 mg tissue was homogenized at high speed for 45 s in 1 mg/100 ml buffer (Phosphate buffered saline: pH 7.5; Triton X-100: 1% v/v; Protease Inhibitor Cocktail and Phosphatase Inhibitor Cocktails #1 and #2: 2x each; DTT: 1 mM; EDTA: 0.5 mM). Aliquots of homogenate were centrifuged at 18,500 × g, 4°C for 45 min and supernatants were normalized to 2.5 μg/ml following protein determination with the BCA assay (Pierce Thermo Scientific, Rockford, Il). Aliquots of normalized supernatant were prepared for SDS-PAGE by addition of 5x Laemmli buffer and incubation at 95°C for 10 min.

2.8. Immunoblots

Protein identification using PAGE-Western Blot was done with adaptations of previously described techniques from this laboratory (Gertzberg et al., 2004; Johnson, 2009; Neumann et al., 2006). Lung homogenates, 20 μg/lane, were separated on 8% polyacrylamide mini-gels, transferred to PVDF membranes (Immobilon-P, Millipore, Bedford, MA), rinsed in TBS (Tris-HCl: 10 mM-pH 7.5; NaCl: 100 mM) and blocked in Blotto + Phosphatase Inhibitors (BPI) (TTBS: [TBS; Tween-20: 0.05%]; nonfat dry milk: 5.0% w/v; NaF: 50 mM; activated Na_3VO_4: 0.1 mM). All antibody incubations were done at room temperature for 1.5 h in BPI unless stated otherwise and each incubation was followed by five 5 min washes in TTBS. The blots were first probed in a mixture of either 1:2500 dilution of anti-phospho-GSK3α/β-$Ser^{21/9}$ (Cell Signaling Technology, Danvers, MA), or 1:2000 anti-phospho-

eNOS-Ser^{1177} rabbit polyclonal antibodies, in 5% BSA in TTBS overnight at 4 °C, followed by incubation in 1:1000 goat anti-rabbit-HRP.

After imaging, the blots were stripped with *Restore PLUS Western Blot Stripping Buffer* (Thermo Scientific), reblocked in BPI, washed, and incubated either 1.5 h at RT or overnight at 4°C in BPI containing a mixture of 1:1000 anti-un-phosphorylated-β-catenin-Ser$^{33/37}$ (clone 8E4, EMD Chemicals, Inc., Gibbstown, NJ) followed by 1:10,000 anti-mouse-HRP. The blots were again stripped after imaging, and reprobed with 1:1000 anti-GSK3α (sc1846, Santa Cruz) goat polyclonal antibody followed by 1:5000 anti-goat-HRP. A 3rd reprobe was 1:10,000 of anti-eNOS, 1:10,000 of anti-β-Catenin (sc7199 Santa Cruz) and 1:2000 anti-GSK3β (sc9166) rabbit polyclonal antibodies. The values for GSK3α and GSK3β activation are noted as the GSK3α/phospho-GSK3α-Ser^{21} and GSK3β/phospho-GSK3β-Ser^{9} ratios because the phosphorylation of GSK3α-Ser^{21} and phospho-GSK3β-Ser^{9} is a modification that decreases the kinase activity of the enzymes (Bhat et al., 2004). Lung lysate was measured for un-phospho-β-catenin-Ser$^{33/37}$ because a decrease in un-phosphorylatied-β-catenin-Ser$^{33/37}$ is a “signature” outcome of increased GSK3α/β activity (Aberle et al., 1997; Daugherty and Gottardi, 2007).

A fourth reprobe was with 1:20,000 mouse anti-β-actin (clone AC74, Sigma), or with 1:5000 rabbit polyclonal anti-PP2a (clone 1512-1; Epitomics, Burlingame, CA) and anti-phospho-PP2a-Tyr ^{307} (Epitomics) followed by incubation in 1:1000 anti-mouse HRP or goat anti-rabbit HRP. The values of PP2a activation are derived from the PP2a/phospho-PP2a-Tyr ^{307} ratios because this phosphorylation inhibits activity of PP2a.

In some studies, an additional reprobe was performed with blots of lung homogenates from FITC-BSA permeability studies with 1:1000 anti-FITC-HRP mouse monoclonal antibody (MAB045P, Millipore).

Biotinylated Protein Ladder Detection Pack (Cell Signaling Technology, Danvers, MA) with either the included goat anti-biotin-HRP at 1:5000 dilution or mouse anti-biotin-HRP (clone BN-34, Sigma) at 1:20,000 was used for in-image MW reference. Imaging substrates used were *Supersignal West Pico* or *West Dura Extended Duration Substrate* (Thermo Scientific) or a combination of the two. Images were acquired on a Kodak Image Station 440CF (Eastman Kodak, Rochester, NY) and analyzed for net band intensity using the ROI threshold method with Kodak 1D software.

2.9. Oxidized protein

The oxidation of amino acid side chains (e.g., amide groups) results in the formation of carbonyl groups and the carbonyls form dinitrophenylhydrazone (DNP) adducts via the Schiff reaction (Levine et al., 2000). Lysates were derivatized to form DNP adducts using the protocol provided by *Oxyblot Oxidized Protein Detection Kit* as previously described by us (S7150KIT; Oncor, Gaithersburg, MD) (Ferro et al., 1997). The DNP adducts were assayed with Western blot using primary polyclonal IgG anti-DNP antibody (Oncor).

2.10. Statistics

A one way analysis of variance (ANOVA) was used to compare values among the treatments. If significance among treatments was noted, a post-hoc multiple comparison test was done with a Holm-Sidak (parametric-equal variance) test to determine significant differences among the groups. A Student T-Test was performed when appropriate. Each lung represents a single experiment. All data are reported as mean ± S.E.M.. Significance was at $P < 0.05$. There are 5–10 samples per group in all studies.

3. RESULTS

3.1. The GSK3β-inhibitors SB216763 and TDZD-8 prevent the TNF-induced increase in vascular permeability (Fig. 1–2)

The purpose of the following studies is to interpret the TNF response integrated with an effect of GSK3α/β-inhibition using SB216763 and TDZD-8. Fig. 1 shows the pulmonary time course of the hemodynamic response in the SB216763 groups with and without TNF-0.5 h, 4.0 h and 24 h. The values were similar among the Control-0.5 h, -4.0 h and -24 h groups, and among the SB-0.5 h, -4.0 h and -24 h groups; therefore, the data was separately combined within the Control and SB-control group. In response to TNF, there was a progressive increase in Ra/Rv because of a progressive decrease in Rv which became significantly different from Control at TNF-24 h, associated with no change in the Ra. The effects of TNF were prevented in the SB216763+TNF group. In response to TNF, there was a progressive decrease in the Ppc which became significantly different from Control at TNF-24 h that can be explained by the associated increase in the Ra/Rv. In response to TNF, there was a progressive increase in the extravascular albumin which became significantly different from Control at TNF-24 h. In response to TNF, there was no change in W-D/D compared to the Control group; however, the W-D/D was greater in the TNF-0.5 h and 24.0 h groups compared to the respective SB216763+TNF groups.

Fig. 1 shows a representative (N=3) anti-FITC immunoblot in the Control and TNF-24 h group that shows only a band at ~66.4 kDa MW indicating there is intact FITC-albumin in the lung lysates.

Fig. 2 shows the experiments using TDZD-8 to verify the protective effect of GSK3α/β-inhibition in the response to TNF. In the TDZD-8+TNF-24 h group, the Ppc, Ra/Rv, Ra and extravascular albumin are similar to the respective values in the TDZD-8 group, and not different from the values in the Control group. In the TDZD-8+TNF-24 h group, the Rv was greater than the value in the Control group. In the TDZD-8+TNF-24 h group, there was a trend for the W-D/D to be less than the value in the TNF-24 h group. The data of Fig. 1–2 indicates that TNF-24 h induces an increase in vascular permeability associated with a decreased Ppc which is prevented by the GSK3α/β inhibitors SB216763 and TDZD-8.

3.2. TNF-4.0 h induces activation of GSK3β (Fig. 3)

TNF-4.0 h lungs were chosen for analysis because 4.0 h was the closest time point preceding the significant rise in the extravascular albumin. Fig. 3 demonstrates a representative Western blot (n=6) of the lung lysate phospho-GSK3α-Ser^{21} and phospho-GSK3β-Ser^{9} in the Control and TNF-4.0 h groups. There is no significant difference in total GSK3α and total GSK3β values among the groups (data not shown). The bar graph is the mean lung lysate values for GSK3α/β activation. In the TNF-4.0 h group, there was no change in the GSK3α activation but there was an increase in GSK3β activation compared to the Control group.

3.3. TNF-4.0 h induces activity of GSK3β-Ser^{9} inhibited by SB216763 (Fig. 4)

In the TNF-4.0 h group, there was a decrease in un-phospho-β-catenin-$Ser^{33/37}$/β-catenin ratio which did not occur in the SB216763 groups, indicating effective inhibition of the TNF-induced increase in GSK3β activity by SB216763. There was no difference in β actin among the groups.

The data of Fig. 3–4 indicate that TNF-4.0 h causes activation of GSK3β that is inhibited by SB216763.

3.4. SB216763 and TDZD-8 prevent the TNF-24 h induced increase in phospho-eNOS-Ser^{1177} and oxidized protein (Fig. 5)

Fig. 5-Panel A demonstrates the mean lung lysate phospho-eNOS-Ser^{1177}/eNOS ratio in the Control, TNF-24, SB216763+ TNF-24 h and TDZD-8+TNF-24 h groups. In the TNF-24 h group, there is an increase in phospho-eNOS-Ser^{1177}/eNOS ratio compared to the Control group which did not occur in the SB216763+TNF-24 h and TDZD-8+TNF-24 h groups.

Fig. 5-panel B demonstrates the mean lung lysate of oxidized protein in the Control, TNF-24 h, SB216763+TNF-24 h and TDZD-8+TNF-24 h groups. In the TNF-24 h group, there is an increase in oxidized protein compared to the Control, SB216763+TNF-24 h and TDZD-8+TNF-24 h groups.

The data of Fig. 5 indicate that GSK3β inhibition prevents TNF-24.0 h induced increases in phospho-eNOS-Ser^{1177}/eNOS and oxidized protein which supports the idea that GSK3β inhibition prevents TNF-induced lung inflammation.

3.5. GSK3α/β in the TNF-24 h group (Fig. 6)

Fig. 6 demonstrates a representative Western blot of lung lysate phospho-GSK3α-Ser^{21} and phospho-GSK3β-Ser^{9} in the Control and TNF-24 h groups. In the TNF-24 h group, there was no difference in activation of GSK3α and GSK3β, compared to the Control group. In the SB216763+TNF-24 h and TDZD-8+TNF-24 h groups, there was decreased activation of GSK3β compared to the Control group.

3.6. SB216763 and TDZD-8 inhibit GSK3α/β activity in the TNF-24 groups (Fig. 7)

In the TNF-24.0 h group, the un-phospho-β-catenin-Ser$^{33/37}$/β-catenin ratio was similar to the Control group; however, the un-phospho-β-catenin-Ser$^{33/37}$/β-catenin ratio was increased in the SB216763+TNF and TDZD-8+TNF groups. There was no difference in β-actin among the groups.

The data of Fig. 6–7 indicate that SB216763 and TDZD-8 can cause persistent inhibition of GSK3α/β in the treated TNF-24.0 h groups despite the return of GSK3α/β activity to baseline levels by 24 h the TNF group.

3.7. TNF cause a decrease in phospho-Ty ^{307} (Table 1)

The altered phosphorylation of GSK3β-Ser ^{9} indicates possible altered activity of PP2a, a Ser/Thr-phosphatase known to regulate GSK3β-Ser ^{9} activity. In the TNF-4.0 h group, there was an increase in PP2a activation compared to the Control group which did not occur in the TNF-24.0 h group.

4.0. Discussion

In the present study, TNF-4.0 h causes an increase in GSK3β activity because there was: (1) an increase in the GSK3β/GSK3β-Ser^{9} ratio, (2) a decrease in un-phosphorylated-β-catenin-Ser$^{33/37}$/β-catenin ratio and (3) inhibition of the decrease in un-phosphorylated-β-catenin-Ser$^{33/37}$ by SB216763 (Konigshoff and Eickelberg, 2010; Masckauchan et al., 2005; van Noort et al., 2002). Importantly, the level of β-actin is similar among all the groups, indicating the effect of TNF is unlikely due to non-specific effects on cell protein.

In the present study TNF-24 h *in vivo* causes an: (1) increase in vascular permeability, (2) increased Ra/Rv, and (3) decreased Ppc in the isolated lung. The lack of TNF-induced increase in the W-D/D was likely due to the moderate increase in endothelial permeability associated with the decrease in Ppc. The structurally dissimilar GSK3α/β inhibitors

SB216763 and TDZD-8 were used to assess the role of GSK3α/β in the response to TNF. The efficacy of SB216763 and TDZD-8 induced GSK3α/β inhibition was verified because SB216763 and TDZD-8 similarly prevented the decrease in un-phosphorylated-β-catenin-Ser$^{33/37}$/β-catenin in the TNF-4.0 and/or TNF-24.0 h groups despite the potential non-specific affects which is inherent in the use of pharmacologic inhibitors such as SB16763 and TDZD-8 (Bain et al., 2007). Finally, in the present experiments SB16763 and TDZD-8 were co-treated with the TNF; thus, the therapeutic efficacy of SB16763 and TDZD-8 (e.g., GSK3α/β inhibitors administered after TNF) remains to be determined.

The literature indicates multiple cell types and mechanisms for the TNF-induced activation of GSK3β in the lung. First, a decrease in PKB (i.e., Akt) mediated phosphorylation of GSK3α/β-Ser$^{21/9}$ will increase GSKα/β activity such as in endothelial cells (Bhat et al., 2004; Dugo et al., 2007b). In pursuing the role of Akt, we determined a significant trend for a decrease in the phospho-Akt-Ser^{473}/Akt ratio which is a post translational modification that would decrease Akt activity (Control: 0.18 ± 0.07 RDU ratio *vs.* TNF: 0.07 ± 0.04 RDU ratio, p=.131). The multiple cell types in the lung may have masked the significant decrease in Akt activity in the TNF-4.0 h group. Second, an increase in PYK2 (Hartigan et al., 2001)-dependent phosphorylation of GSK3α/β-Tyr $^{279/216}$ will activate GSK3α/β, an event that may occur in response to TNF. Third, PP2a is a phosphatase which can de-phosphorylate GSK3α/β-Ser$^{21/9}$, providing activation of the enzyme (Qian et al., 2009). Indeed, the present decrease in PP2a-Tyr^{307} at TNF-4.0 h but not at TNF-24 h indicates activation of the phosphatase correlating with the increase in GSK3β activity in the TNF-4.0 h group with a return to baseline GSK3β activity in the TNF-24 h group. In ongoing studies, our data using TOPflash plasmid transfection detected with immunohistochemistry and luciferase activity, that shows β-catenin mediated expression of luciferase *in vivo*, indicates in lungs isolated from TNF-4.0 h treated rats (0.36±0.05 relative light unit ratio [RLU], N=4), there is significantly decreased (P<0.05) luciferase activity, compared to Control (0.79±0.10 RLU, N=4) and SB216763+TNF-4.0 h (2.59±1.10 RLU, N=4) rats. Mock transfections without the plasmid (N=4) using only transfection reagents indicated zero luciferase activity in the lung. The decreased (i.e., also detected with histochemistry in both endothelial and epithelial cells) activity (i.e., expression) of TOPflash is further evidence that there is greater GSK3β activation in lungs from TNF-treated rats because phospho-β-catenin-Ser $^{33/37}$ is degraded via the proteosome rather than translocating to the nucleus promoting luciferase expression.

To verify the protective effect of SB216763 and TDZD-8 we investigated pathways known to mediate inflammation associated with increased lung vascular permeability. Firstly, in the TNF-24 h group, there is a significant increase in oxidized protein and in phospho-eNOS-Ser^{1177}/eNOS which is a post-translational modified activated form of eNOS, compared to the Control group. We previously showed *in vitro* that TNF-induced eNOS activation via nitric oxide causes endothelial injury and protein oxidation (Ferro et al., 1997). In addition, we showed that nitric oxide enhances injury in lungs isolated from TNF treated guinea pigs (Johnson and Ferro, 1996). In the present study, SB216763 and TDZD-8 prevents the increase in phospho-eNOS-Ser^{1177}/eNOS and oxidized protein consistent with the idea that increased GSK3α/β activity via eNOS activation promotes vascular injury associated with inflammation (Cuzzocrea et al., 2006; Ferro et al., 1997). Similarly, Cuzzocrea et al showed that the carrageen-induced nitration of tyrosine residues and the lung injury is suppressed by inhibition of GSK3α/β implicating a nitric oxide dependent pathway (Cuzzocrea et al., 2006). Secondly, in the present study, GSK3α/β-inhibition using SB216763 and TDZD-8 caused an increase in un-phosphorylated-β-catenin-Ser$^{33/37}$. It is well demonstrated that activation of GSK3α/β decreases β-catenin by forming increased phosphorylated-β-catenin-Ser$^{33/37}$ which is degraded by the proteosome (Aberle et al., 1997; Hagen et al., 2002). Thus, in the present study the preserved β-catenin can re-incorporate to adherence junctions promoting maintenance of endothelial barrier function a concept that is under investigation

in our laboratory (van Noort et al., 2002; Venkiteswaran et al., 2002). Thirdly, in the present study, GSK3α/β-inhibition using SB216763 and TDZD-8 prevented the TNF-24 h-induced decrease in Ppc. Nitric oxide promotes the low pressure profile in our previous guinea pig model of TNF-induced increased constriction and lung edema despite contributing to lung injury (Ferro et al., 1993; Johnson and Ferro, 1992). The suppression of GSK3α/β activity may decrease the release of reactive nitrogen species, thus normalizing the decreased Ppc. The literature clearly supports the concept that GSK3α/β promotes eNOS derived nitric oxide generation (Cheng et al., 2009; Huang et al., 2009) during lung injury but the pathways are not clearly defined requiring further investigation (Cuzzocrea et al., 2006). Interestingly, in the present study, GSK3β activity returned to baseline values by 24.0 h; however, the treatment with SB216763 and TDZD-8 persistently reduced the GSK3β activity because of the effected increase in un-phosphorylated-β-catenin-$Ser^{33/37}$/β-catenin (Konigshoff and Eickelberg, 2010; Masckauchan et al., 2005; van Noort et al., 2002). In addition, treatment with SB216763 and TDZD-8 increased phospho-GSK3β-Ser^{9} in the TNF groups. Similarly, in a variety of models for inflammation, SB216763 and TDZD-8 have been shown to increase phospho-GSK3β-Ser^{9} associated with decreased GSK3β activity via yet to be described pathways (Aberle et al., 1997; Ang et al., 2009; Bove et al., 2001; Daugherty and Gottardi, 2007; Eldar-Finkelman et al., 2009; Johnson and Ferro, 1996; Neumann et al., 2006); however, inhibition of GSK3β-Ser^{9} dependent activation of PP2a may prevent the feed-forward continued activation of GSK3β.

The assessment of eNOS and oxidized protein at the peak of the permeability response reflects “downstream” activity of GSK3β during lung injury. There is compartment and time dependent co-localization of activated GSK3α/β with substrates such as β-catenin (e.g., membrane vs nucleus) and eNOS (e.g., membrane vs. cytosol) that can promote differences in the time course for detection of phosphorylation events downstream of GSK3β activity (Dugo et al., 2007a; Dugo et al., 2007b; Zhou et al., 2009). Interestingly, most substrates for GSK3α/β require a priming phosphorylation, via a different kinase, a site which is four residues distant from the site for GSK3β phosphorylation (Aberle et al., 1997; Daugherty and Gottardi, 2007; Frame et al., 2001; van Noort et al., 2002). The primed phosphorylated residue of the substrate interacts with a docking site-Arg^{96} in GSK3β rendering the substrate ready for phosphorylation; however, β-catenin is reported not to require the docking site (Aberle et al., 1997; Daugherty and Gottardi, 2007; Eldar-Finkelman et al., 2009; Frame et al., 2001). The above events will invariably impact the time-course for detection of outcomes of GSK3α/β activity (e.g., β-catenin, eNOS, oxidized protein) that regulate the increase in endothelial permeability induced by TNF-24 h (Aberle et al., 1997; Ang et al., 2009; Bove et al., 2001; Daugherty and Gottardi, 2007; Eldar-Finkelman et al., 2009; Johnson and Ferro, 1996; Neumann et al., 2006).

In summary, TNF induces the activation of GSK3β associated with lung injury. The pharmacologic inhibition of GSK3α/β with SB216763 and TDZD-8 prevents TNF-induced increases in the markers of lung endothelial injury which are vascular permeability and oxidized protein. The development of strategies that target GSK3α/β may provide novel directions for therapy of acute respiratory distress syndrome and lung inflammation.

Acknowledgments

I want to thank Paul H. Neumann and Nancy Gertzberg for their extraordinary technical assistance. The experiments were supported by NHLBI RO1-HL-59901 (A. Johnson).

References

Aberle H, Bauer A, Stappert J, Kispert A, Kemler R. beta-catenin is a target for the ubiquitin-proteasome pathway. Embo J. 1997; 16:3797–3804. [PubMed: 9233789]

Ang AD, Adhikari S, Ng SW, Bhatia M. Expression of nitric oxide synthase isoforms and nitric oxide production in acute pancreatitis and associated lung injury. Pancreatology. 2009; 9:150–159. [PubMed: 19077466]

Bain J, Plater L, Elliott M, Shpiro N, Hastie CJ, McLauchlan H, Klevernic I, Arthur JS, Alessi DR, Cohen P. The selectivity of protein kinase inhibitors: a further update. Biochem J. 2007; 408:297–315. [PubMed: 17850214]

Bhat RV, Budd Haeberlein SL, Avila J. Glycogen synthase kinase 3: a drug target for CNS therapies. J Neurochem. 2004; 89:1313–1317. [PubMed: 15189333]

Bove K, Neumann P, Gertzberg N, Johnson A. Role of ecNOS-derived NO in mediating TNF-induced endothelial barrier dysfunction. Am J Physiol Lung Cell Mol Physiol. 2001; 280:L914–922. [PubMed: 11290515]

Cheng YL, Wang CY, Huang WC, Tsai CC, Chen CL, Shen CF, Chi CY, Lin CF. Staphylococcus aureus induces microglial inflammation via a glycogen synthase kinase 3beta-regulated pathway. Infect Immun. 2009; 77:4002–4008. [PubMed: 19596777]

Cuzzocrea S, Crisafulli C, Mazzon E, Esposito E, Muia C, Abdelrahman M, Di Paola R, Thiemermann C. Inhibition of glycogen synthase kinase-3beta attenuates the development of carrageenan-induced lung injury in mice. Br J Pharmacol. 2006; 149:687–702. [PubMed: 17016509]

Daugherty RL, Gottardi CJ. Phospho-regulation of Beta-catenin adhesion and signaling functions. Physiology (Bethesda). 2007; 22:303–309. [PubMed: 17928543]

Dugo L, Collin M, Allen DA, Patel NS, Bauer I, Mervaala E, Louhelainen M, Foster SJ, Yaqoob MM, Thiemermann C. Inhibiting glycogen synthase kinase 3beta in sepsis. Novartis Found Symp. 2007a; 280:128–142. discussion 142–126, 160–124. [PubMed: 17380792]

Dugo L, Collin M, Thiemermann C. Glycogen synthase kinase 3beta as a target for the therapy of shock and inflammation. Shock. 2007b; 27:113–123. [PubMed: 17224784]

Eichacker PQ, Hoffman WD, Farese A, Banks SM, Kuo GC, MacVittie TJ, Natanson C. TNF but not IL-1 in dogs causes lethal lung injury and multiple organ dysfunction similar to human sepsis. J Appl Physiol. 1991; 71:1979–1989. [PubMed: 1761500]

Eldar-Finkelman H, Licht-Murava A, Pietrokovski S, Eisenstein M. Substrate Competitive GSK-3 Inhibitors strategy and Implications. Biochim Biophys Acta. 2009

Ferro TJ, Gertzberg N, Selden L, Neumann P, Johnson A. Endothelial barrier dysfunction and p42 oxidation induced by TNF-alpha are mediated by nitric oxide. Am J Physiol. 1997; 272:L979–988. [PubMed: 9176264]

Ferro TJ, Hocking DC, Johnson A. Tumor necrosis factor-alpha alters pulmonary vasoreactivity via neutrophil-derived oxidants. Am J Physiol. 1993; 265:L462–471. [PubMed: 8238533]

Frame S, Cohen P, Biondi RM. A common phosphate binding site explains the unique substrate specificity of GSK3 and its inactivation by phosphorylation. Mol Cell. 2001; 7:1321–1327. [PubMed: 11430833]

Fujisawa N, Hayashi S, Kurdowska A, Noble JM, Naitoh K, Miller EJ. Staphylococcal enterotoxin A-induced injury of human lung endothelial cells and IL-8 accumulation are mediated by TNF-alpha. J Immunol. 1998; 161:5627–5632. [PubMed: 9820542]

Gertzberg N, Neumann P, Rizzo V, Johnson A. NAD(P)H oxidase mediates the endothelial barrier dysfunction induced by TNF-alpha. Am J Physiol Lung Cell Mol Physiol. 2004; 286:L37–48. [PubMed: 12807699]

Hagen T, Di Daniel E, Culbert AA, Reith AD. Expression and characterization of GSK-3 mutants and their effect on beta-catenin phosphorylation in intact cells. J Biol Chem. 2002; 277:23330–23335. [PubMed: 11967263]

Hartigan JA, Xiong WC, Johnson GV. Glycogen synthase kinase 3beta is tyrosine phosphorylated by PYK2. Biochem Biophys Res Commun. 2001; 284:485–489. [PubMed: 11394906]

Hocking DC, Phillips PG, Ferro TJ, Johnson A. Mechanisms of pulmonary edema induced by tumor necrosis factor-alpha. Circ Res. 1990; 67:68–77. [PubMed: 2114228]

Huang WC, Lin YS, Wang CY, Tsai CC, Tseng HC, Chen CL, Lu PJ, Chen PS, Qian L, Hong JS, Lin CF. Glycogen synthase kinase-3 negatively regulates anti-inflammatory interleukin-10 for lipopolysaccharide-induced iNOS/NO biosynthesis and RANTES production in microglial cells. Immunology. 2009; 128:275–286.

Johnson A. TNF-induced activation of pulmonary microvessel endothelial cells: a role for GSK3beta. Am J Physiol Lung Cell Mol Physiol. 2009; 296:L700–709. [PubMed: 19218353]

Johnson A, Ferro TJ. TNF-alpha augments pulmonary vasoconstriction via the inhibition of nitrovasodilator activity. J Appl Physiol. 1992; 73:2483–2492. [PubMed: 1490962]

Johnson A, Ferro TJ. Nitrovasodilator repletion increases TNF-alpha-induced pulmonary edema. J Appl Physiol. 1996; 80:2151–2155. [PubMed: 8806924]

Konigshoff M, Eickelberg O. WNT signaling in lung disease: a failure or a regeneration signal? Am J Respir Cell Mol Biol. 2010; 42:21–31. [PubMed: 19329555]

Laux H, Tomer R, Mader MT, Smida J, Budczies J, Kappler R, Hahn H, Blochinger M, Schnitzbauer U, Eckardt-Schupp F, Hofler H, Becker KF. Tumor-associated E-cadherin mutations do not induce Wnt target gene expression, but affect E-cadherin repressors. Lab Invest. 2004; 84:1372–1386. [PubMed: 15311212]

Lee HB, Blaufox MD. Blood volume in the rat. J Nucl Med. 1985; 26:72–76. [PubMed: 3965655]

Lee YH, Suzuki YJ, Griffin AJ, Day RM. Hepatocyte growth factor regulates cyclooxygenase-2 expression via beta-catenin, Akt, and p42/p44 MAPK in human bronchial epithelial cells. Am J Physiol Lung Cell Mol Physiol. 2008; 294:L778–786. [PubMed: 18245266]

Levine RL, Wehr N, Williams JA, Stadtman ER, Shacter E. Determination of carbonyl groups in oxidized proteins. Methods Mol Biol. 2000; 99:15–24. [PubMed: 10909073]

Masckauchan TN, Agalliu D, Vorontchikhina M, Ahn A, Parmalee NL, Li CM, Khoo A, Tycko B, Brown AM, Kitajewski J. Wnt5a signaling induces proliferation and survival of endothelial cells in vitro and expression of MMP-1 and Tie-2. Mol Biol Cell. 2006; 17:5163–5172. [PubMed: 17035633]

Masckauchan TN, Shawber CJ, Funahashi Y, Li CM, Kitajewski J. Wnt/beta-catenin signaling induces proliferation, survival and interleukin-8 in human endothelial cells. Angiogenesis. 2005; 8:43–51. [PubMed: 16132617]

Meijer L, Flajolet M, Greengard P. Pharmacological inhibitors of glycogen synthase kinase 3. Trends Pharmacol Sci. 2004; 25:471–480. [PubMed: 15559249]

Miura T, Miki T. GSK-3beta, a therapeutic target for cardiomyocyte protection. Circ J. 2009; 73:1184–1192. [PubMed: 19506320]

Neumann P, Gertzberg N, Vaughan E, Weisbrot J, Woodburn R, Lambert W, Johnson A. Peroxynitrite mediates TNF-alpha-induced endothelial barrier dysfunction and nitration of actin. Am J Physiol Lung Cell Mol Physiol. 2006; 290:L674–L684. [PubMed: 16284212]

Qian W, Shi J, Yin X, Iqbal K, Grundke-Iqbal I, Gong CX, Liu F. PP2A Regulates Tau Phosphorylation Directly and also Indirectly via Activating GSK-3beta. J Alzheimers Dis. 2010; 19:1221–1229. [PubMed: 20308788]

Schafer R, Abraham D, Paulus P, Blumer R, Grimm M, Wojta J, Aharinejad S. Impaired VE-cadherin/beta-catenin expression mediates endothelial cell degeneration in dilated cardiomyopathy. Circulation. 2003; 108:1585–1591. [PubMed: 12963640]

van Noort M, Meeldijk J, van der Zee R, Destree O, Clevers H. Wnt signaling controls the phosphorylation status of beta-catenin. J Biol Chem. 2002; 277:17901–17905. [PubMed: 11834740]

Venkiteswaran K, Xiao K, Summers S, Calkins CC, Vincent PA, Pumiglia K, Kowalczyk AP. Regulation of endothelial barrier function and growth by VE-cadherin, plakoglobin, and beta-catenin. Am J Physiol Cell Physiol. 2002; 283:C811–821. [PubMed: 12176738]

Zhou XW, Winblad B, Guan Z, Pei JJ. Interactions Between Glycogen Synthase Kinase 3beta, Protein Kinase B, and Protein Phosphatase 2A in Tau Phosphorylation in Mouse N2a Neuroblastoma Cells. J Alzheimers Dis. 2009; 17:929–937. [PubMed: 19542610]

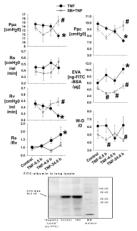

Fig. 1. The pulmonary hemodynamics in the Control and SB216763 groups with and without TNF

Figure 1 is the mean data of Ppa, Ra, Rv, Ra/Rv Ppc, extravascular albumin (EVA) and W/D in the Control (N=19), TNF-0.5 h (N=9), TNF-4.0 h (N=9), TNF-24 h (N=5), SB216763 (N=12), SB216763+TNF-0.5 h (N=7), SB216763+TNF-4.0 h (N=7) and SB216763+TNF-24 h (N=5) groups. The Ppc is assessed with the double occlusion technique. The EVA is the extravascular FITC-albumin measured in lung homogenate. All measurements are taken following a baseline steady state.

*= different (P< 0.05) from the Control using the ANOVA with Holm-Sidak post-hoc multiple comparison test.

#= different (P< 0.05) from the TNF group using the ANOVA with Holm-Sidak post-hoc multiple comparison test.

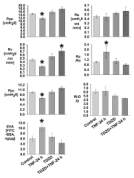

Fig. 2. The pulmonary hemodynamics in the Control and TDZD-8 groups with and without TNF-24 h

Figure 2 is the mean data of Ppa, Ra, Rv, Ra/Rv, Ppc, extravascular albumin (EVA) and W/D in the Control (N=19), TNF-24 h (N=5), TDZD-8 (N=5) and TDZD+TNF-24 h (N=5) groups. The Ppc is assessed with the double occlusion technique. The EVA is the extravascular FITC-albumin measured in lung homogenate. All measurements are taken following a baseline steady state.

*= different ($P < 0.05$) from the Control using the ANOVA with Holm-Sidak post-hoc multiple comparison test.

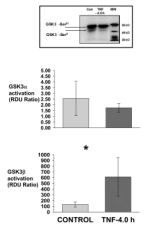

Fig. 3. TNF-4.0 h-induces activation of GSK3β

Lung lysate is assessed for phospho-GSK3α-Ser^{21}, GSK3α, phospho-GSK3β-Ser^{9} and GSK3β in the Control (N=14), TNF-4.0 h (N=6), SB216763 (N=6) and SB216763+TNF-4.0 h (N=6) groups. A representative Western blot is shown. The data is expressed as GSK3α/β activation (Relative Density Units [RDU] ratio) derived from GSK3α/phospho-GSK3α-Ser ^{21}and GSK3β/phospho-GSK3β-Ser^{9}.

*= different (P< 0.05) from the Control group using the ANOVA with Holm-Sidak post-hoc multiple comparison test.

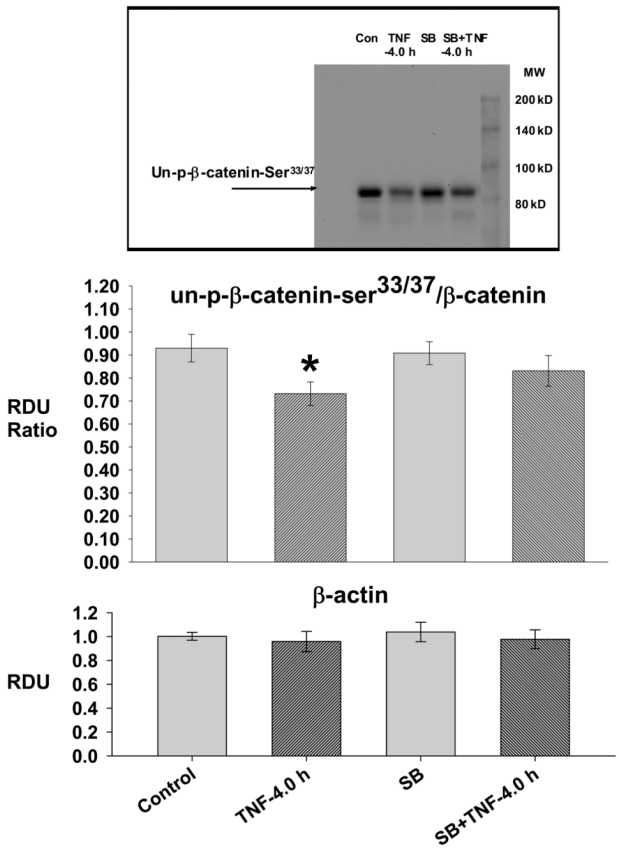

Fig. 4. TNF-4.0 h causes increased GSK3β activity

Lung lysate is assessed for un-phospho-β-catenin$^{33/37}$, β-catenin and β-actin in the Control (N=14), TNF-4.0 h (N=6), SB216763 (SB, N=6) and SB216763+TNF-4.0 h (N=6) groups. A representative Western blot is shown. The data is expressed as the un-phospho-β-catenin$^{33/37}$/β-catenin (RDU ratio).

*= different (P< 0.05) from the Control group using the ANOVA with Holm-Sidak post-hoc multiple comparison test.

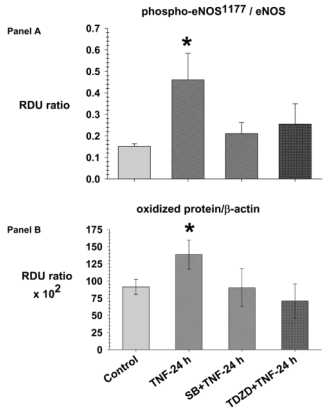

Fig. 5. TNF causes phosphorylation of eNOS-Ser^{1177} and increased oxidized protein prevented by SB216763 and TDZD-8

Lung lysate is assessed for phospho-eNOS-Ser^{1177}, total eNOS (panel A) and oxidized protein (panel B) in the Control (N=4), TNF-24 h (N=4), SB216763 (SB) +TNF-24 h (N=4) and TDZD-8 (TDZD)+TNF-24 h (N=4) groups. Lysates were derivatized to form dinitrophenylhydrazone adducts (DNP). The DNP adducts were assayed with Western blot using primary polyclonal IgG anti-DNP antibody. The data is expressed as the phospho-eNOS-Ser^{1177}/eNOS and oxidized protein/β-actin (RDU ratio).

*= different ($P < 0.05$) from the Control group using the ANOVA with Holm-Sidak post-hoc multiple comparison test.

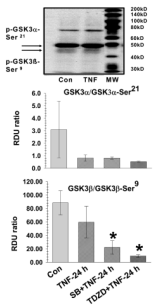

Fig. 6. SB216763 and TDZD-8 reduce GSK3β activation in the TNF-24 h groups

Lung lysate is assessed for phospho-GSK3α-Ser^{21}, GSK3α, phospho-GSK3β-Ser^{9} and GSK3β in the Control (N=14), TNF-24.0 h (N=6), SB216763 (SB)+TNF-24 h (N=6) and TDZD-8 (TDZD)+TNF-24 h (N=4) groups. A representative Western blot is shown for the Control, TNF-24.0 h groups. The data is expressed as GSK3α/β activation (Relative Density Units [RDU] ratio) derived from GSK3α/phospho-GSK3α-Ser ^{21} and GSK3β/phospho-GSK3β-Ser ^{9}.

*= different (P< 0.05) from the Control group using the ANOVA with Holm-Sidak post-hoc multiple comparison test.

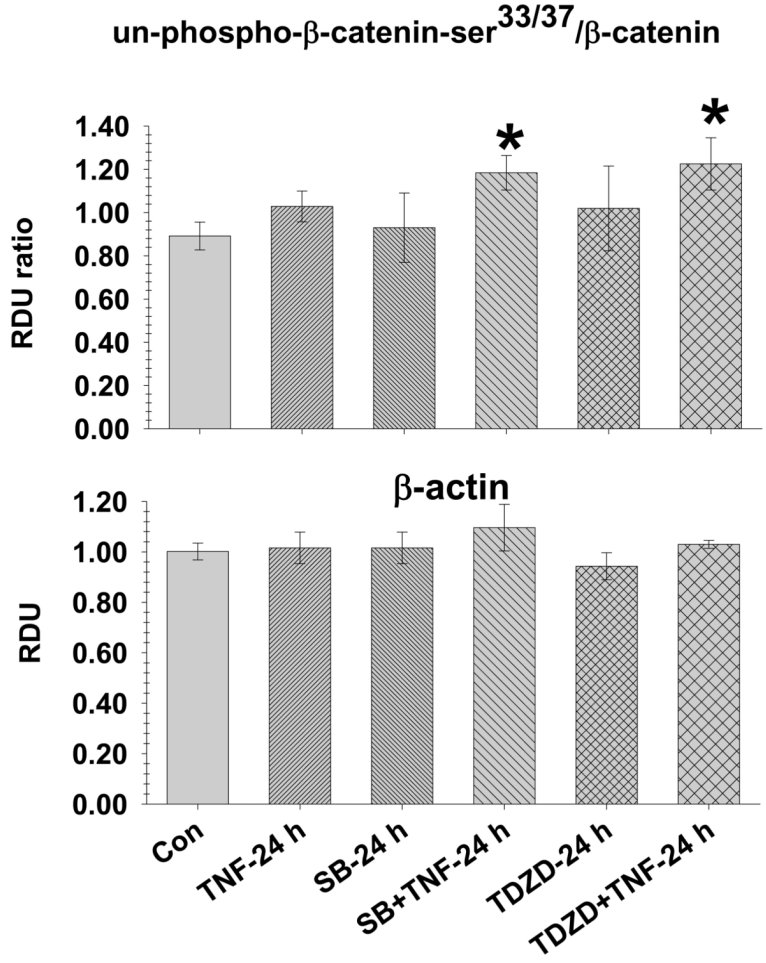

Fig. 7. SB216763 and TDZD-8 inhibit GSK3β activity at TNF-24 h

Lung lysate is assessed for un-phospho-β-catenin$^{33/37}$, β-catenin and β-actin in the Control (N=14), TNF-24.0 h (N=8), SB216763 (SB)+TNF-24 h (N=6) and TDZD-8 (TDZD) +TNF-24 h (N=4) groups. The data is expressed as the un-phospho-β-catenin$^{33/37}$/β-catenin (RDU ratio).

*= different (P< 0.05) from the Control group using the ANOVA with Holm-Sidak post-hoc multiple comparison test.

Table 1

	PP2a/phospho-PP2a-Tyr307 (RDU ratio)
Control (N=6)	1.9+0.5
TNF-4.0 h (N=6)	3.2+0.2[a]
TNF-24 h (N=5)	2.4+0.3

[a] significantly different from Control, P<0.05.